

## VLBI imaging and optical variability of the BL Lac object OQ 530 (B1418+546)<sup>★</sup>

E. Massaro<sup>1,2</sup>, F. Mantovani<sup>3</sup>, R. Fanti<sup>3,4</sup>, M. Maesano<sup>5</sup>, F. Montagni<sup>5</sup>, R. Nesci<sup>1</sup>,  
S. Sclavi<sup>1</sup>, G. Tosti<sup>6</sup>, and T. Venturi<sup>3</sup>

<sup>1</sup> Dipartimento di Fisica, Università di Roma “La Sapienza”, Piazzale A. Moro 2, 00185 Roma, Italy  
e-mail: [enrico.massaro@uniroma1.it](mailto:enrico.massaro@uniroma1.it)

<sup>2</sup> IASF - Sez. di Roma, via del Fosso del Cavaliere 100, 00133 Roma, Italy

<sup>3</sup> Istituto di Radioastronomia, viale P. Gobetti 101, 40129 Bologna, Italy

<sup>4</sup> Dipartimento di Fisica, Università di Bologna, via Irnerio 46, 40126 Bologna, Italy

<sup>5</sup> Stazione Astronomica di Vallinfreda, Vallinfreda (RM) Italy

<sup>6</sup> Oss. Astronomico and Dipartimento di Fisica, Università di Perugia, via A. Pascoli, 06123 Perugia, Italy

Received 27 February 2004 / Accepted 12 May 2004

**Abstract.** Results of VLBI and optical observations are presented for the BL Lac object OQ 530 (B1418+546), whose long term optical variability is characterised by a decreasing mean luminosity trend. EVN images at 1.6 GHz and 5 GHz of OQ 530 show a very bright core with a much weaker jet extending to about 35–40 mas. The radio flux density from the core in June 2001 was much higher than that measured in February 1999. A similar increase was also found from nearly simultaneous optical photometry, while the total flux density of the jet remained unchanged. The structure of the jet shows several knots which move outward with an apparent superluminal motion with a  $\beta_{\text{app}} \geq 3.5h^{-1}$ . The region within about 3 mas from the core contains a component not well resolved in our images and emerging from it in the jet direction. That component was also detected in images taken from 1990 to 1997 and it seems to be a rather stable structural feature. Using nearly simultaneous optical and radio data, we can describe the SED of the synchrotron peak with a simple formula, approximating a power law at low frequencies and a log-parabola at the high ones, whose maximum lies in the range  $3.5\text{--}5 \times 10^{13}$  Hz, and the extrapolation in the X-ray range gives a flux comparable to that observed with BeppoSAX.

**Key words.** galaxies: active – galaxies: BL Lacertae objects: individual: OQ 530 – galaxies: jets

### 1. Introduction

The emission from BL Lacertae objects, which covers the entire electromagnetic spectrum from radio frequencies to the  $\gamma$  rays, is characterized by large amplitude variations over a wide range of time scales from minutes to years. Fast variability and high apparent luminosity are explained by synchrotron radiation from a Doppler boosted relativistic bulk motion of high energy electrons moving down a jet closely aligned to the line of sight (Blandford & Rees 1978). VLBI images of many BL Lac objects have shown the presence of polarised jets emerging from a compact core along which knots move with superluminal speeds, which are large for most  $\gamma$ -ray loud sources (Marscher & Marchenko 1999; Jorstad et al. 2001). For a few sources, for which historic optical light curves are available, luminosity variations have been observed over a very wide interval of time scales ranging from days up to several decades. Assuming that the same electron population is

emitting in the optical and radio bands by synchrotron mechanism, one can expect that the occurrence of these variations can be associated either with structural changes of the inner jet or with variations of the core flux density, likely detectable with VLBI observations. Recently, Savolainen et al. (2002) showed that in a sample of 27  $\gamma$ -ray blazars there is a connection between the outburst detected from the total flux density light curves at 22 GHz and 37 GHz and VLBI components emerging into the jet.

To test this hypothesis we started a program of high resolution radio imaging of the two bright BL Lac objects ON 231 and OQ 530 (B1418+546;  $z = 0.152$ ) whose historic optical light curves show secular trends of their mean brightness (Tosti et al. 1999; Nesci & Massaro 1999). Superposed to the long term changes, variations over time scales of weeks to months and amplitudes of  $\sim 1.5\text{--}2$  mag were frequently observed. Images of ON 231, whose mean luminosity was increasing for about 20 years, were obtained just after the large optical burst of April 1998 and showed the presence of new components (Massaro et al. 2001). After that burst, this source entered in a slow dimming phase of the optical luminosity

<sup>★</sup> Table A.1 is only available in electronic form at the CDS via anonymous ftp to [cdsarc.u-strasbg.fr](ftp://cdsarc.u-strasbg.fr) (130.79.128.5) or via <http://cdsweb.u-strasbg.fr/cgi-bin/qcat?J/A+A/423/935>

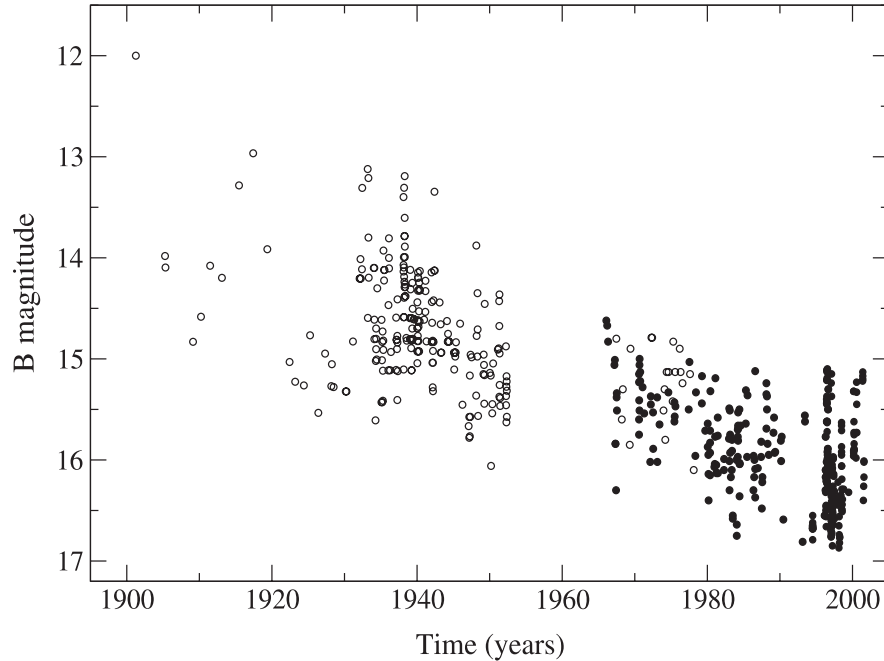


**Fig. 1.** The historic optical light curve of OQ 530, derived from archive data (open circles, Miller 1978) corrected according Nesci & Massaro (1999), and updated with other measurements from the Asiago archive and from our monitoring program (filled circles).

(Tosti et al. 2002), suggesting that a rather stable modification may have occurred in that occasion.

In this paper we describe the optical behaviour of OQ 530 since 1995, derived from our photometric monitoring, and we present new images at 1.6 and 5.0 GHz collected from 1998 to 2001 with the European VLBI Network (EVN)<sup>1</sup>. Previous VLBI images at 5 GHz of OQ 530, obtained in 1990 (Xu et al. 1995), 1992 (Gabuzda et al. 1999) and 1996 (Fomalont et al. 2000), can be used to follow its structure evolution in relation to the luminosity changes. Furthermore, a series of images at 8.4 GHz taken in 1997 can be found in the Radio Reference Frame Image Database (RRFID) (Fey & Charlot 2000). Three high resolution images at 22 GHz obtained from observations taken from November 1992 to October 1996 are given by Wiik et al. (2001).

## 2. Optical observations

The historic optical light curve of OQ 530 in the photometric *B* band, taken from Nesci & Massaro (1999) and updated with more recent observations, is reported in Fig. 1. The data until 1977 were obtained by Miller (1978) from the Harvard archive plates. Those after that date are based upon our work on the Asiago archive and photometric monitoring. An offset correction has been applied to the Miller (1978) unfiltered photographic magnitudes to match the Asiago mean value (see Nesci & Massaro 1999, for details). This light curve shows that the mean luminosity was fading since the beginning of the past

century when the source was very bright ( $B \approx 12$ ). The lowest brightness was likely reached in the mid of the last decade, when OQ 530 varied around a mean level  $B \approx 16.5$ . In recent years an increase of the mean optical luminosity of OQ 530 has been observed. After February 2000 its mean magnitude remained brighter than in the previous months suggesting a change in the trend of the light curve.

Optical photometry of OQ 530 was performed with the 0.5 m reflector of the Astronomical Station of Vallinfreda (Rome), the Automatic 0.4 m reflector AIT of the Perugia University Observatory, and with a 0.35 m Newtonian telescope at Greve, near Florence. Other data were obtained with the TRC70 (0.70 m) telescope at Monte Porzio, near Rome. All these instruments are equipped with CCD cameras and standard Johnson *B*, *V* and Cousins *R*, *I* bandpasses. Aperture photometry was made with IRAF-apphot using several reference stars in the same field of the sources, whose *V*, *R*, *I* magnitudes are given by Fiorucci & Tosti (1996); *B* values were retrieved from Miller et al. (1984), however they were affected by a systematic offset of 0.1 mag, which was included in our analysis. Zero magnitude fluxes were taken from Mead et al. (1990). Our first photometric data of OQ 530 were taken in 1994–1995 and a more continuous monitoring started in 1996. The resulting light curve in the *R* band is plotted in Fig. 2 (upper panel), while all the data in the four bands are given in Appendix (Table A.1).

In the first part of the light curve the typical magnitude of OQ 530 was around  $R \approx 15.3$ , and only on the occasion of a flare observed in August 1996 it brightened up to  $R = 14.2$ . A rather faint phase, in which the source was only occasionally brighter than  $R = 15$  but generally fainter than 15.5, lasted about three years from the beginning of 1997 to the end of

<sup>1</sup> The European VLBI Network is a joint facility of European, Chinese, South African and other radio astronomy institutes funded by their national research councils.

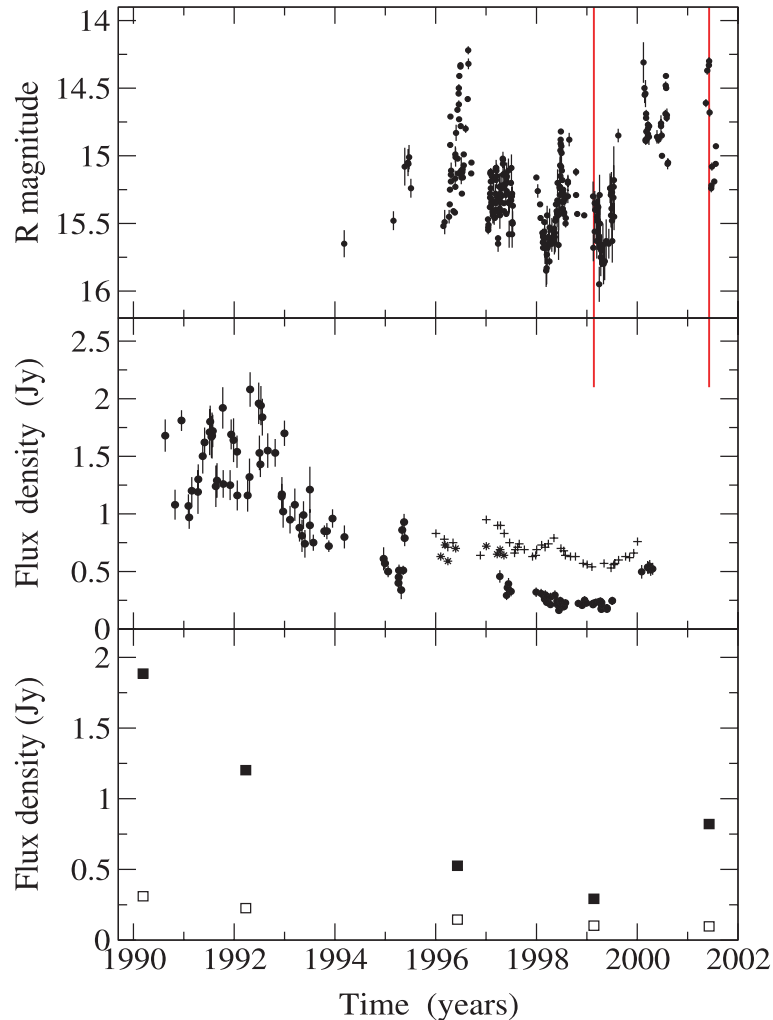


**Fig. 2.** *Upper panel:* the optical light curve in the *R* (Cousins) band of OQ 530 from 1994 to 2001. *Central panel:* light curves of OQ 530 at several radio and submillimetric frequencies; data at 22 GHz to May 1995 (solid circles) are taken from (Teräsraanta et al. 1998) and those from 1996 to 1997 (asterisks) from (Venturi et al. 2001); data at 8.4 GHz (1996–2000, crosses) are also from (Venturi et al. 2001) and those at 353 GHz (open circles) are from (Robson et al. 2001). *Lower panel:* time history of the core (filled squares) and the jet (open squares) flux density at 5 GHz of OQ 530 derived from literature and from our observations. The two vertical solid (grey) lines indicate the epoch of our VLBI observations at 5 GHz (1999, Feb. 20 and 2001, June 5).

1999. In particular, the lowest level was reached in March 1999 ( $R \approx 15.9$ ). After that epoch OQ 530 showed a decrease of the mean magnitude. Bright states were observed in February and July 2000 and another maximum at  $R = 14.3$  occurred on 4 June 2001, almost simultaneous with our last VLBI observations.

The BL Lac nucleus of OQ 530 is hosted in a bright galaxy whose properties have been studied by several authors (Abraham et al. 1991; Stickel et al. 1993; Wurtz et al. 1996; Scarpa et al. 2000) and more recently by Pursimo et al. (2002). From their data it is possible to estimate the *R* magnitude of the host galaxy within a photometric diameter of  $5''$  in the range 16.3–17.0. We computed the flux of the nuclear component after the subtraction of the host galaxy contribution for which we assumed the typical colours of an elliptical galaxy (Fukugita et al. 1995) and considered the corresponding *k*-correction. The resulting host galaxy fluxes in the four photometric bands were:  $F(B) = 0.13$ ,  $F(V) = 0.41$ ,  $F(R) = 0.64$  and  $F(I) = 1.07$  mJy.

### 3. Long-term radio behaviour

To have a more complete description of the activity of OQ 530 in the past years in the central panel of Fig. 2 we plot the monitoring data in the radio and submillimetric bands as reported in literature. For the period from 1990 to 1995 the flux measurements at 22 GHz performed with the Metsähovi radio telescope (Teräsraanta et al. 1998) are available. Data at the same frequency up to May 1997 are given by Venturi et al. (2001), who also performed a monitoring programme at 8.4 GHz until January 2000. In the same panel are also plotted the flux density data at the wavelength of  $850 \mu\text{m}$  (353 GHz) obtained with the James Clerk Maxwell Telescope by Robson et al. (2001). The 22 GHz data from 1990 to 1995 show that in 1995 the mean flux was about one third of that in 1991–92, as for the VLBI core fluxes (see below). The subsequent decrease of the radio flux to 1999 is furthermore confirmed by the two monitoring programmes in the radio (Venturi et al. 2001) and in the submillimetric bands (Robson et al. 2001). As it happened in

**Table 1.** ENV observations of OQ 530.

Array	Date	Stations*	Term. (Mode)	Freq. GHz	Band MHz	Correlator	Int. time s
EVN	08 Jun. 1998	Ef, Cm, Sm, Jb-1, Mc, Nt, On-85, Ur, Wb	MK3A (A)	1.6	56	MPIfR, Bonn	4.0
EVN	20 Feb. 1999	Cm, Jb-2, Mc, Nt, On-85, Ur, Wb, Sh, Tr	MK3A (B)	5.0	28	MPIfR, Bonn	4.0
EVN	05 Jun. 2001	Ef, Cm, Jb-2, Mc, Nt, On-85, Sh, Wb, Tr	MKIV	5.0	64	JIVE, Dwingeloo	2.0

\* Cm Cambridge 32 m; EF Effelsberg 100 m; Jb-1 Lovell 76 m; Jb-2 Mk2 25 m; Mc Medicina 32 m; Nt Noto 32 m; On-85 Onsala 25 m; Sh Shanghai 25 m; Sm Simeiz 22 m; Tr Torun 32 m; Ur Urumqi 25 m; Wb Westerbork array  $N \times 25$ .

the optical, after that epoch the source started a brightening phase.

#### 4. VLBI-EVN observations

VLBI images of OQ 530 were obtained during three observing sessions scheduled by the European VLBI Network (EVN). The related information are summarized in Table 1. In particular, the two 5 GHz images were taken in 1999 and 2001 during the faint and bright optical period, respectively, as indicated by the vertical lines in Fig. 2.

The raw data outputs from the correlators were calibrated in amplitude and phase using AIPS and imaged using DIFMAP (Shepherd et al. 1995). Total power measurements taken at the same times as the VLBI observations and the gain curve of the telescopes were applied in the amplitude calibration process. The self-calibration procedure, which uses closure amplitude to determine telescope amplitude corrections, gave calibration factors that were generally within 10% of unity for all the telescopes available along the observing sessions and only in a couple of cases the calibration factors were in the range 15–20%.

The parsec-scale structure of OQ 530 is characterized by a low brightness well-defined jet emerging from a compact bright core at  $PA \approx 127^\circ$ . This structure is clear in both the two high sensitivity EVN 5 GHz images of February 1999 (Fig. 3) and June 2001 (Fig. 4) and in the image at 1.6 GHz (Fig. 5). The jet has an extension of about 40 mas and shows a complex structure with several components. The two images at 5 GHz are presented using a convolution beam of  $4 \times 2 \text{ mas}^2$  at  $PA 0^\circ$ . It is worth mentioning that the present observations suffer for a poor  $u$ - $v$  plane coverage mainly in the East-West direction due to the gap between the European and the Chinese telescopes. Moreover, for the June 05, 2001 observations the  $u$ - $v$  coverage is also degraded by the lack of detection of fringes for the baselines involving the Urumqi station.

Starting from February 2000 we observed a brightness increase of the mean optical luminosity of about a magnitude. A strong activity of the source core was also detectable in the radio band, as it clearly appears in the two images presented here. We measured an increase of the flux density at 5 GHz by a factor of  $\sim 3$ , from 292 mJy in February 1999 to 821 mJy in June 2001 (see the modelfitting given in Table 2). In the optical database we have photometric information nearly simultaneous with the June 2001 observations. Precisely, we measured  $R_C = 14.30$  on 4 June 2001. We do not have simultaneous data

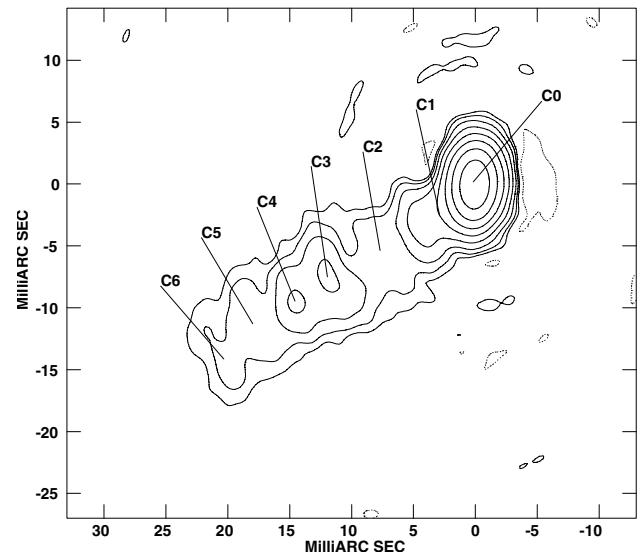


**Fig. 3.** The EVN image of OQ530 at 5 GHz (February 20, 1999). The contour levels are  $-1, 1, 2, 4, 8, 16, 32, 64, 128 \text{ mJy}$ . The peak flux density is  $233.1 \text{ mJy beam}^{-1}$ . The beam is  $4 \times 2 \text{ mas}^2$  at  $PA 0^\circ$ .

for the former EVN observations. The closest  $R_C$  magnitudes are  $15.67 \pm 0.10$  (February 16) and  $15.40 \pm 0.09$  (February 26). Therefore we assume the intermediate value of 15.5 as indicative of the optical brightness at the epoch of VLBI observations. These data, shown in the SEDs of Fig. 7, indicate that about the same factor was found for the variations in the radio and optical bands, suggesting that the same electron population is responsible for the synchrotron radiation in the core region in both these bands.

To describe the structure of the jet at the two epochs, we fitted the images with a number of Gaussian components. The modelfitting process has been done using DIFMAP, which makes use of the closure phases. The results are given in Table 2, where for each component we report the flux density, the radial distance from the core  $R$  and the Position Angle measured from the North direction, the major axis  $A$ , the axial ratio and the orientation. We verified that the total fluxes derived from these models agree with those derived integrating over the entire source extension in the hybrid image, with an accuracy better than 2%. We also verified that the images obtained transforming back the input model nicely reproduce the hybrid images. Note, however, that the total flux density from the jet

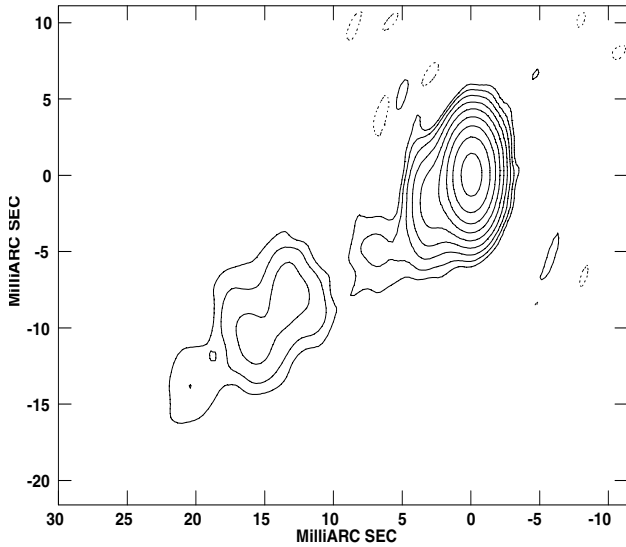


**Fig. 4.** The EVN image of OQ530 at 5 GHz (June 05, 2001). The contour levels are  $-2, 2, 4, 8, 16, 32, 64, 128, 256, 512$  mJy. The peak flux density is  $712.0 \text{ mJy beam}^{-1}$ . The beam is  $4 \times 2 \text{ mas}^2$  at PA  $0^\circ$ .

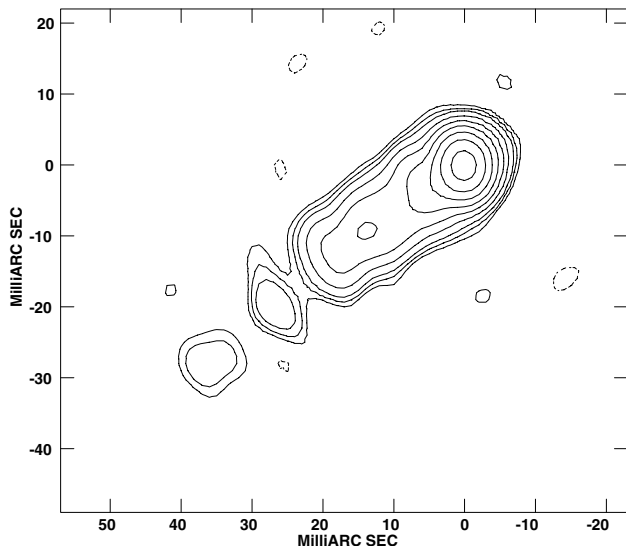


**Fig. 5.** The EVN image of OQ530 at 1.67 GHz (June 08, 1998). The contour levels are  $-1.5, 1.5, 2.5, 4, 8, 16, 32, 64, 128, 256$  mJy. The peak flux density is  $363.6 \text{ mJy beam}^{-1}$ . The beam is  $5.8 \times 4.6 \text{ mas}^2$  at PA  $14^\circ$ .

components ( $\sim 100$  mJy) is about the same at the two epochs. In Fig. 6 we plot the intensity profiles along the jet taken from the two 5 GHz images. The extension of the jet is about 25–30 mas in both profiles.

Two interesting common features can be noticed in the two 5 GHz images, i.e. the structure of the core and the two main jet components. In both images the core shows an elongated emission in the direction of the jet extending up to about 4 mas from the centre position, as if a new jet component was originating from it. The model fittings give actually the presence of a component, indicated by C1 in Table 2, which appears as a bump on the east side of the core in the profiles of Fig. 6. The proximity of the much stronger C0 may affect the parameters estimated for C1 in both models. The flux density values at

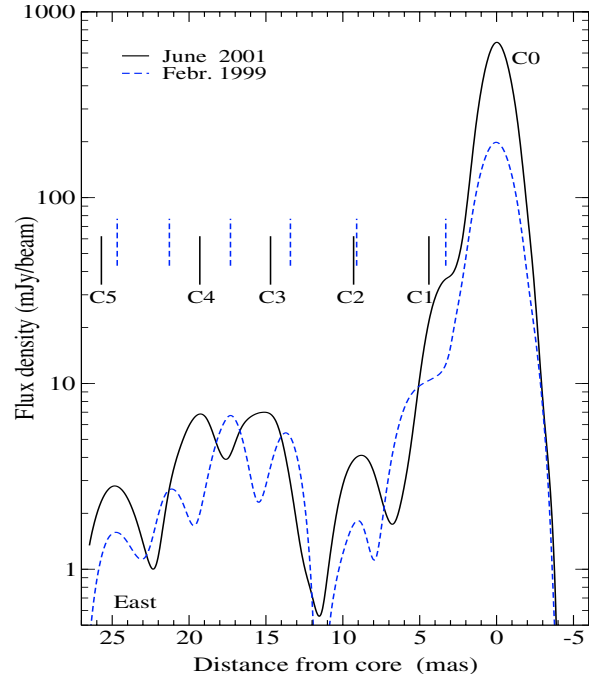


**Fig. 6.** The flux density profiles along the jet of OQ 530 at the frequency of 5 GHz. The flux scale is logarithmic to view better the low brightness features. The vertical lines indicate the positions of the components given by the model fittings in Table 2.

**Table 2.** Model fitting of the 5 GHz images of OQ 530.

Comp.	Flux density (mJy)	$R$ (mas)	PA (deg)	$A$ (mas)	Axial ratio	$\phi$ (deg)
1999 Feb.						
C0	291.8	0.0	0.00	1.3	0.69	$-7.54$
C1	41.4	3.3	116.3	2.5	0.35	25.2
C2	8.5	9.1	126.8	2.9	0.80	120.3
C3	24.7	13.4	126.0	4.5	0.51	36.2
C4	14.1	17.3	121.0	2.8	0.50	36.3
C5	8.6	21.3	123.7	2.0	0.54	35.2
C6	3.0	24.7	127.5	1.0	1.00	0.0
2001 June						
C0	820.9	0.0	0.0	1.2	0.50	$-42.7$
C1	42.2	4.4	123.0	1.6	0.43	$-5.0$
C2	3.5	9.3	133.3	2.1	0.83	34.0
C3	23.5	14.7	122.0	2.2	0.70	57.5
C4	25.2	19.3	123.0	2.0	0.63	$-5.1$
C5	5.1	25.7	125.1	1.0	1.00	0.0

Note: components are ordered from West to East.

the two epochs are about the same ( $\sim 40$  mJy) suggesting little luminosity evolution. The three previous published images of the inner jet of OQ 530 at 5 GHz (Xu et al. 1995; Gabuzda et al. 1999; Fomalont et al. 2000) show the same core dominated structure. All those images were made with a slightly higher resolution than ours, and the model fittings require additional components within 1.5 mas from the core. A component at a distance of about 1.5 mas from the core is also seen in the Global VLBI images at 22 GHz of September 1993 and

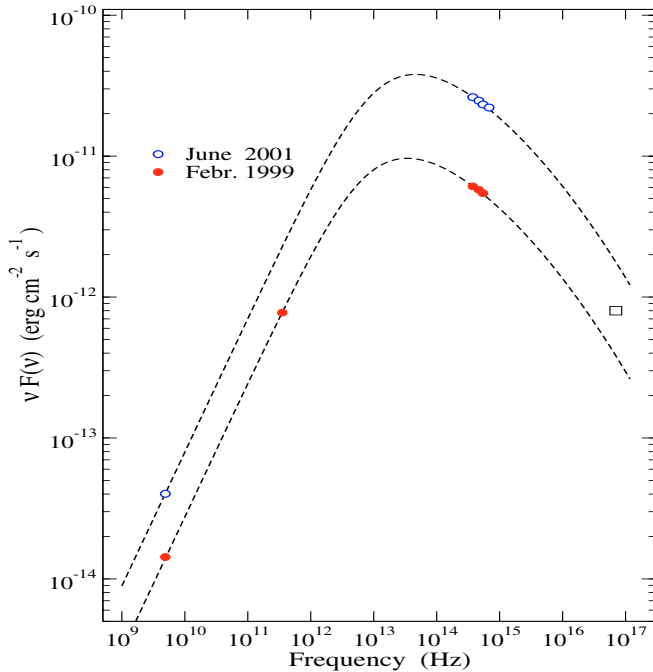


**Fig. 7.** Two possible SEDs of synchrotron core emission of OQ 530 covering the radio to X-ray range. Optical data are from our database. Open square is the flux at 0.5 keV measured by BeppoSAX in March 2000. Dashed lines are the SED modeled using the law of Eq. (2).

October 1996 by Wiik et al. (2001). Furthermore, a component at about 2 mas is visible in the RRFID images taken in 1997 at 8.4 GHz (Fey & Charlot 2000). All these results indicate that in addition to the strong core there is evidence for a relatively bright emission very near to it (<2 mas). It is not clear if we are observing a new born knot or a stationary component as discussed in the next section.

We carefully check for any indication of the presence of a secondary component in the core region in the imaging and modelfitting processes. As pointed out by Savolainen et al. (2002), a clear correlation exists between a strong increase in the core flux density, as that found here, and the appearance of a new born component in the nucleus. The model for the June 2001 observations of Table 2, nicely fits the closure phases triangles in general and those involving the longest baselines, in our case between the European antennas and Shanghai, in particular. So, we are not requested to use more than one component to model the nucleus, as it was found necessary by Savolainen et al. (2002) in similar cases, to allow a better fit between model and closure phases calculated for the longest baselines. Moreover, the full resolution beam is  $2.8 \times 0.9 \text{ mas}^2$  at PA =  $-31.4^\circ$ , with the major axis which is almost in the direction of the jet. Such observational constraints limit our ability to model the core region with more than one component.

To compare the flux densities measured in our observations with those reported in the literature quoted above, we used the modelfitting given by these authors and added the flux densities of the components within an angular separation of 1.5 mas from the core. We found that the core flux density decreased from about 1.9 Jy in 1990 to 0.29 Jy in 1999. It is interesting to note that also the flux density of the jet,

obtained by adding the flux densities of the individual components, decreased from 0.31 in 1990 Jy to 0.1 in 1999 (Fig. 2, lower panel).

The other jet features (components C2 to C5) are fainter and lie at distances of 10 to 20 mas from the core. Note the presence of two resolved maxima (components C3 and C4) with a flux density of  $\sim 20$  mJy. We associated the same numbered components detected in the two images to estimate their proper motion. From the data of Table 2 (see also Fig. 6) we found the outward displacements of 1.4, 2.0 mas for C3 and C4, respectively. The displacement of C2 cannot be established and it is compatible with zero: it is the weakest component and its position can be affected by the local jet emission. Also the proper motion of C5 is uncertain because it is not clear which of the two outer components of February 1999 it can be associated with. The apparent velocity, measured in units of the speed of light, is evaluated by means of the usual formula (see, for instance, Pearson & Zensus 1987):

$$\beta_{\text{app}} = \frac{\mu z}{2.2 \times 10^{-2} h (1+z)} \frac{1 + \sqrt{1+z} + z}{1 + \sqrt{1+z} + z/2} = 6.21 \frac{\mu}{h} \quad (1)$$

where  $\mu$  is the proper motion in mas/yr,  $q_0$  has been taken equal to 0.5 and  $h = H_0/100 \text{ km s}^{-1} \text{ Mpc}^{-1}$ . The resulting values of  $\beta_{\text{app}}$  are then in the interval  $3.8h^{-1} - 5.4h^{-1}$ , in agreement with those estimated by Gabuzda et al. (1999). This result confirms the superluminal motion of the components along the jet, with a possible outward acceleration.

## 5. Discussion

### 5.1. The spectral energy distribution

The Spectral Energy Distribution (SED) of BL Lac objects, and generally Blazars, is characterized by two broad peaks. The peak at lower frequency (S peak) is explained by synchrotron emission from high energy electrons, while the one at higher frequencies (IC peak) is due to inverse Compton scattering from the same electron population (Maraschi et al. 1992). Padovani & Giommi (1995) introduced a classification of BL Lac object based on the frequency of the S peak: LBL (Low-energy peaked BL Lacs) if the maximum of the S peak lies in the interval  $10^{12} - 10^{14}$  Hz, and HBL (High-energy peaked BL Lacs) if it lies above  $10^{16}$  Hz.

The new EVN images of OQ 530 and the monitoring results presented here provide a strong indication that optical luminosity changes are associated with similar variations of the radio emission from the core. This suggests that the synchrotron emission from the core consists of a single components whose spectrum covers a very wide frequency interval from the radio band to the UV and, likely, to X-rays. A simple, but likely realistic, model of the SED can be given by the following analytic law:

$$F(\nu) = K \nu^{-(a+b \text{Log}(1+\nu/\nu_1))} \quad (2)$$

which for  $\nu \ll \nu_1$  it coincides with a power law of spectral index  $a$ , while for  $\nu \gg \nu_1$  it changes to a log-parabolic law. This spectral shape is justified by an energy dependent statistical acceleration, as proposed by Massaro et al. (2004) to explain the

log-parabolic spectra observed in some BL Lac sources. In this framework Eq. (2) can be originated from a constant acceleration probability for particles of low energy and from a decreasing probability when the particle energy becomes higher than a critical value. In Fig. 7 we present two possible SEDs of OQ 530 corresponding to the low luminosity state of the core observed in February 1999 and to the brighter one observed in June 2001. The optical data are taken from our database (Table A.1): for the not strictly simultaneous measurements of February 1999 we have only  $R$  and  $I$  data and therefore the fluxes in  $B$  and  $V$  were derived using the mean source colours. For the former epoch we found in the literature a nearly simultaneous measurement at 353 GHz (Robson et al. 2001) which is useful to constrain the low frequency power law. For June 2001 observation the lack of data from the millimetric to the near IR bands does not allow a good description of the SED and consequently we assume the same spectral shape.

The values of the parameters  $a = 0.05$  and  $b = 0.08$  are the same for the two distributions of Fig. 7, while the frequency  $\nu_1$  is equal to  $7.4 \times 10^{12}$  Hz for the SED of February 1999 and to  $1.1 \times 10^{13}$  Hz for that of June 2001. The factor  $K$  changed by a factor of 2.9 between the two epochs as the ratio of the core fluxes in Table 2. The peak frequencies of the two SEDs are  $3.5 \times 10^{13}$  in 1999 and  $4.8 \times 10^{13}$  Hz in 2001, in the infrared range, as expected for a LBL object.

We stress that, because of the small number of observational points, these distributions are only indicative of the true ones. However, the X-ray fluxes extrapolated by these laws are not in disagreement with the BeppoSAX measurement reported by Tagliaferri et al. (2003) from an observation taken on 26–27 March 2000. The fact that the high energy tail of the S peak can extend up to the keV range is a consequence of the low value of the parameter  $b$ , which measures the spectral curvature (see Massaro et al. 2004), while in some other BL Lac sources  $b$  was found in the interval 0.11–0.18 (Perri et al. 2003). This result explains why OQ 530 was classified by Tagliaferri et al. (2003) as an “intermediate” BL Lac object on the basis of its X-ray spectrum, while it is more properly a LBL source.

## 5.2. The radio core structure

An interesting problem concerns the structure of the radio core of OQ 530. As discussed in Sect. 3, in our images the core appears to be elongated in the jet direction and the model fitting indicates the presence of a component at a distance of  $\sim 3$  mas, but it could be closer. A component at about 1–2 mas is always detectable in previous images at any of the observing frequencies and therefore it seems a rather “stable” feature. The fact that this distance is about the same despite the fact that the epochs of the observations differ by several years, could be interpreted in many ways. A first hypothesis is that rapidly evolving components are frequently originated in the core. If the radiative cooling time of electrons is short enough, such a new component remains bright only when it is close to the core.

A second interesting possibility is that of the presence of a stationary component. In their extensive VLBI study on a

sample of 42  $\gamma$ -ray loud blazars, Jorstad et al. (2001) found stationary components, within a distance of 2 mas from the core, in 27 sources. They proposed that those components could be associated with a standing hydrodynamical compression. In such case, as discussed in Jorstad et al. (2001), a blend of components in a single feature may occur, which does not show any significant change in its proper motion. An observational strategy to discriminate between the two possible interpretations given above is to plan for simultaneous radio interferometric and optical monitoring observations. The radio observations should be made with VLBI at high frequencies ( $\geq 8.4$  GHz) to gain in resolution and they should be done with a time sampling of  $\sim 1$  year. Such an observing plan will provide information on the non-thermal activity in the core of OQ 530. If the increasing brightness trend noticed since the beginning of 2000 continues in the next years, the radio flux density of OQ 530 may reach again  $\sim 2$  Jy, as it was at the beginning of the past decade, making it a very easy target source for such a VLBI monitoring programme.

## 6. Conclusions

The main results obtained for the BL Lac object OQ 530 and presented in this paper are:

1. OQ 530 presents a historic optical light curve with a decreasing trend. The lower level was reached in March 1999 with  $R \approx 15.9$  when the brightness started increasing again.
2. A similar trend was observed in several radio frequencies.
3. VLBI observations show a well-defined core-jet structure with the jet extending up to  $\approx 40$  mas from the core.
4. VLBI observations at 5 GHz taken in February 1999 and June 2001 show an increase of a factor  $\approx 3$  in the flux density of the core, while the flux density from the whole jet remained constant.
5. The nearly simultaneous photometric observations show that the optical magnitude changed from  $R_C = 15.50$  to  $R_C = 14.30$  in the same period.
6. These data indicate about the same variation factor in the radio and optical bands, suggesting that the same electron population can be responsible for the synchrotron radiation coming from the core region at the two bands.
7. Superluminal motion was detected along the jet with apparent velocities for the components ranging from  $\beta_{\text{app}} = 3.8h^{-1}$  to  $\beta_{\text{app}} = 5.4h^{-1}$ , similar to those found by Gabuzda et al. (1999).
8. The existence of a stationary component at 1–2 mas from the core is suggested and explained either as: i) rapidly evolving components are frequently originated in the core; ii) standing hydrodynamical compression (Jorstad et al. 2001).
9. Two possible Spectral Energy Distributions are derived for the core synchrotron emission at the two observing epochs.
10. OQ 530 can be classified as a Low-energy peaked BL Lac with an unusually mild spectral curvature.

*Acknowledgements.* Part of this work was performed with the financial support Italian MIUR (Ministero dell’ Istruzione Università e Ricerca) under the grant Cofin 2001/028773. The European

VLBI Network is a joint facility of European and Chinese radio astronomy institutes funded by their national research councils. This research was supported by the European Commission's TMR Programme "Access to Large-scale Facilities", under contract No. ERBFMGECT950012. We acknowledge the support of the European Community – Access to Research Infrastructure action of the Improving Human Potential Programme.

## Appendix

In this appendix we report the Table A.1 which contains all the data of our photometric monitoring OQ 530 in the four bands *B*, *V* (Johnson) and *R*, *I* (Cousins) from 1994 to 2001. Table A.1 is available in electronic (ASCII) form at CDS. For each observation we report the observation date (Col. 1), the UT time (Col. 2), the Julian Day (Col. 3), the magnitude (Col. 4) and its error (Col. 5), the photometric band (Col. 6) and the used telescope (Col. 7). The telescope codes are: VA: Vallinfreda, GR: Greve, PG: AIT Perugia, MP: TRC70 Monte Porzio.

## References

- Abraham, R. G., McHardy, I. M., & Crawford, C. S. 1991, *MNRAS*, 252, 482
- Blandford, R. D., & Rees, M. J. 1978, *Phys. Scr.*, 17, 265
- Fey, A. L., & Charlot, P. 2000, *ApJS*, 128, 17
- Fomalont, E. B., Frey, S., Paragi, Z., et al. 2000, *ApJS*, 131, 95
- Gabuzda, D. C., & Cawthorne, 1996, *MNRAS*, 283, 759
- Gabuzda, D. C., Pushkarev, A. B., & Cawthorne, 1999, *MNRAS*, 307, 725
- Jorstad, S. G., Marscher, A. P., Mattox, J. R., et al. 2001, *ApJS*, 134, 181
- Maraschi, L., Ghisellini, G., & Celotti, A. 1992, *ApJ*, 397, L5
- Marscher, A. P., & Marchenko, S. G. 1999, *BL Lac Phenomenon*, ed. L. O. Takalo, & A. Sillanpää, *PASP Conf. Ser.*, 159, 417
- Massaro, E., Mantovani, F., Fanti, R., et al. 2001, *A&A*, 374, 435
- Massaro, E., Perri, M., Giommi, P., & Nesci, R. 2004, *A&A*, 413, 489
- Mead, A. R. G., Ballard, K. R., Brand, P. W. J. L., et al. 1990, *A&AS*, 83, 183
- Miller, H. R. 1978, *ApJ*, 223, L67
- Miller, H. R., Wilson, J. W., Africano, J. L., & Quigley, R. J. 1984, *A&AS*, 57, 353
- Nesci, R., & Massaro, E. 1999, in *Proc. Treasure-Hunting Astronomical Plate Archives*, ed. P. Kroll, C. La Dous, & H.-J. Brauer (Sonneberg), 111
- Padovani, P., & Giommi, P. 1995, *ApJ*, 444, 567
- Pearson, T. J., & Zensus, J. A. 1987, in *Superluminal Radio Sources*, ed. J. A. Zensus, & T. J. Pearson (Cambridge Univ. Press), 1
- Perri, M., Massaro, E., Giommi, P., et al. 2003, *A&A*, 407, 453
- Pursimo, T., Nilsson, K., Takalo, L. O., et al. 2002, *A&A*, 381, 810
- Robson, E. I., Stevens, J. A., & Jenness, T. 2001, *MNRAS*, 327, 751
- Scarpa, R., Urry, M. C., Falomo, R., et al. 2000, *ApJ*, 532, 740
- Shepherd, M. C., Pearson, T. J., & Taylor, G. B. 1995, *BAAS*, 26, 987
- Savolainen, T., Wiik, K., Valtaoja, E., et al. 2002, *A&A*, 394, 851
- Stickel, M., Fried, J. W., & Kühn, H. 1993, *A&AS*, 374, 431
- Tagliaferri, G., Ravasio, M., Ghisellini, G., et al. 2003, *A&A*, 400, 477
- Teräsraanta, H., Tornikoski, M., Mujunen, A., et al. 1998, *A&AS*, 132, 305
- Tosti, G., Fiorucci, M., Luciani, M., et al. 1999, *BL Lac Phenomenon*, ed. L. O. Takalo, & A. Sillanpää, *PASP Conf. Ser.*, 159, 149
- Tosti, G., Massaro, E., Nesci, R., et al. 2002, *A&A*, 395, 11
- Venturi, T., Dallacasa, D., Orfei, A., et al. 2001, *A&A*, 379, 755
- Wiik, K., Valtaoja, E., & Leppänen, K. 2001, *A&A*, 380, 72
- Wurtz, R., Stocke, J. T., & Yee, H. K. C. 1996, *ApJS*, 103, 109
- Xu, W., Readhead, A. C. S., Pearson, T. J., et al. 1995, *ApJS*, 99, 297